Growth of Half-Meter Long Carbon Nanotubes Based on Schulz–Flory Distribution

Rufan Zhang,[†] Yingying Zhang,[‡,*] Qiang Zhang,[†] Huanhuan Xie,[†,‡] Weizhong Qian,[†] and Fei Wei[†,*]

[†]Beijing Key Laboratory of Green Chemical Reaction Engineering and Technology, Department of Chemical Engineering, Tsinghua University, Beijing 100084, China, and [‡]Center for Nano and Micro Mechanics, Tsinghua University, Beijing 100084, China

ABSTRACT The Schulz–Flory distribution is a mathematical function that describes the relative ratios of polymers of different length after a polymerization process, based on their relative probabilities of occurrence. Carbon nanotubes (CNTs) are big carbon molecules which have a very high length-to-diameter ratio, somewhat similar to polymer molecules. Large amounts of ultralong CNTs have not been obtained although they are highly desired. Here, we report that the Schulz–Flory distribution can be applied to describe the relative ratios of CNTs of different lengths produced with a floating chemical vapor deposition process, based on catalyst activity/deactivation probability. With the optimized processing parameters, we successfully synthesized 550-mm-long CNTs, for which the catalyst deactivation probability of a single growth step was ultralow. Our finding bridges the Schulz–Flory distribution and the synthesis of one-dimensional nanomaterials for the first time, and sheds new light on the rational design of process toward controlled production of nanotubes/nanowires.

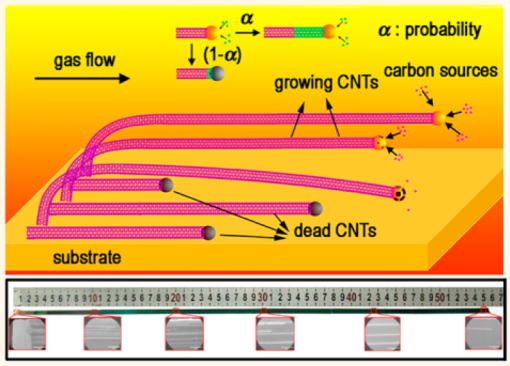

KEYWORDS: carbon nanotubes · ultralong · chemical vapor deposition · Schulz–Flory distribution · catalyst activity

The Schulz–Flory (SF) distribution[1−5] describes the relative ratios of linear condensation polymers of different length after a kinetics-controlled polymerization process, where the monomers are assumed to be equally reactive. The SF distribution can be expressed as $P_x = p^{x-1}(1-p)$, where P_x is the mole fraction of polymers containing x segments (x-mers), p is the probability that each monomer reacts to link to the growing polymer chains, and $(1-p)$ is the probability that no linkage exists. The form of this distribution implies that shorter polymers are favored over longer ones. The SF distribution has been widely accepted to study the distribution of linear condensation polymers[3,4] and even carbon fibers.[6,7]

Carbon nanotubes (CNTs), a typical one-dimensional carbon molecule, are one of the strongest materials ever known.[8−10] The extraordinary mechanical properties of CNTs renders them promising candidates for superstrong fibers, ballistic armors, and even space elevators.[11] Mass production of CNTs with macroscopical length is the first step to realize their application. Gas-flow-directed chemical vapor deposition on silicon substrates is the most effective method to prepare ultralong CNTs,[12−17] and significant progress has been made in the synthesis of ultralong CNTs.[13,18,19] However, the reported longest CNT was only 20 cm,[17] and the number density of ultralong CNTs is usually lower than several CNTs per 100 μm.[12,13,15−17,20] Besides, their number density decreases rapidly along the axial directions (see Figure S1 in Supporting Information).[13,15,17,21−23] Various interpretations were proposed for the growth mechanism of ultralong CNTs.[14,20,24] However, it remains a question why their number density decreases so rapidly and how to synthesize meter-long CNTs.

Theoretically, the growth of horizontally aligned ultralong CNTs fits with the prerequisites of SF distribution,[2,3] which are (i) the carbon source molecules having equal activity, (ii) the polymerization being a kinetics-controlled process, and (iii) having stable

* Address correspondence to yingyingzhang@tsinghua.edu.cn, wf-dce@tsinghua.edu.cn.

Received for review April 22, 2013 and accepted June 27, 2013.

Published online June 27, 2013
10.1021/nn401995z

growth state. It has been widely accepted that the growth of CNTs obeys a screw-dislocation-like mechanism,[25−28] according to which the carbon dimers integrate repetitively into the growing edges of the growing CNTs,[25,28] forming a spiral linear carbon "polymer" (Supporting Information, Figure S2). Wen[17] and Marchand *et al.*[26] have proven that the growth speed of ultralong CNTs is constant at given conditions, clearly indicating the growth of ultralong CNTs is a kinetics-controlled process. Besides, no matter for what kind of carbon sources, it is well understood that all molecules of carbon source are equally reactive to form CNTs.

Herein, we report that the growth of ultralong CNTs can be well interpreted using SF distribution. The size and number distribution of ultralong CNTs is controlled by catalyst activity probability, and can be expressed by SF distribution. The catalyst activity probability plays a key role in the growth of ultralong CNTs and can be tuned by varying the growing parameters. With the optimized conditions, half-meter-long CNTs with perfect structures were available through a process with an high catalyst activity probability.

RESULTS AND DISCUSSION

On the basis of SF distribution, the probability (p) that each monomer reacts to link to the growing polymer chains is the key issue determining the size distribution of linear polymers. Similarly, we can define the probability that each carbon dimer integrates into the growing edge of CNTs. However, it cannot be obtained directly due to the technical limitations and it is not suitable to describe the length distribution of CNTs based on carbon dimers. It is well-known that catalysts play a key role in the growth of ultralong CNTs. On the one hand, despite the difference between factors such as catalyst,[29] substrates,[23,30] feedstock,[17,31] gas velocity,[14] temperature,[12,18] *etc.*, the common point is that all of them have direct or indirect impact on catalyst activity, which accordingly influences the growth of CNTs. On the other hand, the growth of CNTs only depends on whether the catalyst is active and whether the carbon supply is sufficient. Thus, given sufficient carbon supply, the growth of ultralong CNTs can be explored from the viewpoint of catalyst activity.

Figure 1 panels a and b show the tip-growth of ultralong CNTs with catalyst nanoparticles on their tips. The as-grown CNTs are few-walled ones, such as single-walled, double-walled, and triple-walled (Supporting Information, Figure S3). It is a probability event whether a catalyst keeps active during the CNT growth (Figure 1a,c). We define α as the probability that a catalyst particle keeps active enough to maintain a CNT adding a unit length (we choose "1 mm" as a unit length in the following text). Thus α can be called *catalyst activity probability*, while $(1 - \alpha)$ can be called *catalyst deactivation probability*. Figure 1d shows the growing speed of ultralong CNTs keeping constant, indicating their growth is a kinetics-controlled process. Thus we can take α as a constant. According to SF distribution, the percentage (P_L) of CNTs with length L can be expressed as following (for details see Supporting Text S1):

$$P_L = \alpha^{(L-1)}(1 - \alpha) \quad (1)$$

The CNT number density (d_L) at the distance L from the starting position of a substrate is defined as the total percentage of CNTs with length $\geq L$:

$$d_L = \sum_{L}^{\infty} P_L = \alpha^{(L-1)} \quad (2)$$

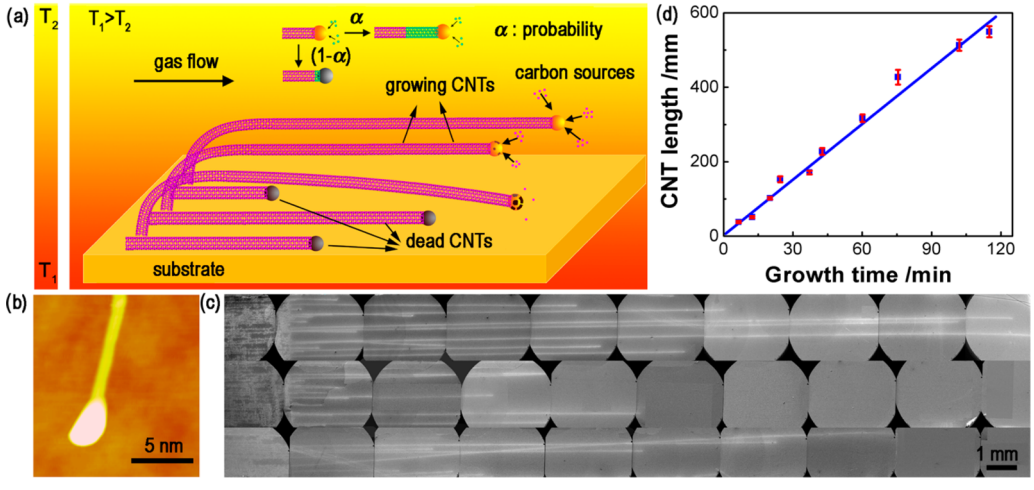

Figure 1. Growth of ultralong CNTs. (a) Illustration of tip-growth of ultralong CNTs. (b) Atomic force microscopy (AFM) image of a CNT with a catalyst nanoparticle on its tip. (c) Mosaic scanning electron microscopy (SEM) images of ultralong CNTs. (d) Relationship between the average CNT length and their growth time. For CNTs with different length on substrates, only the longest 10 CNTs were taken into consideration for calculating growth speed. The average length of the 10 CNTs were taken as the CNT length at a given growth time.

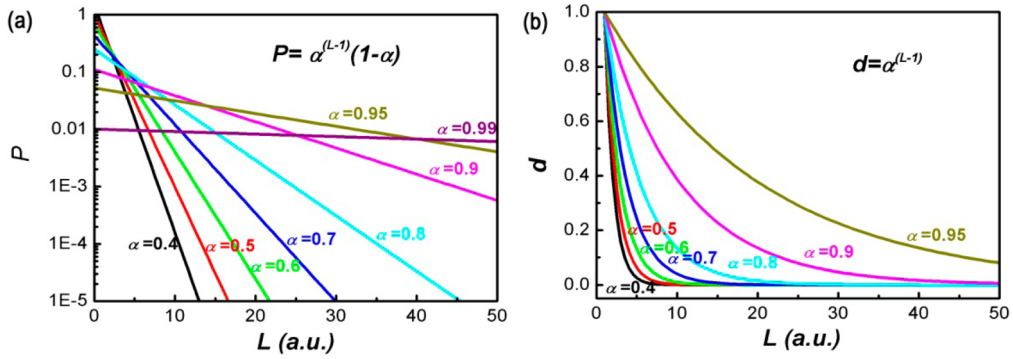

Figure 2. Theoretical number distribution of ultralong CNTs. (a) Theoretical percentage of ultralong CNTs. (b) Theoretical number density of ultralong CNTs.

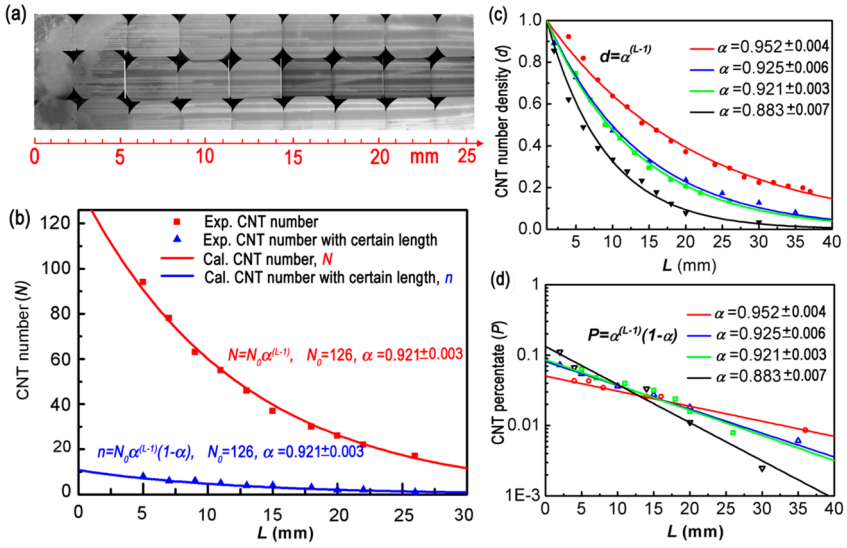

Figure 3. Number distribution of ultralong CNTs. (a) Mosaic SEM images of as-grown ultralong CNTs. (b) Number distribution of CNTs shown in panel a. (c) Number density of ultralong CNTs with four different α. (d) Percentage of ultralong CNTs with four different α.

From eq 1 and 2, we obtain

$$\alpha = 1 - \frac{P_L}{d_L} \quad (3)$$

Although it is difficult to directly measure α, we can obtain the value of α from the ratio of P_L to d_L according to eq 3.

Define N_0 as the total CNT number at the starting position of a substrate, the total CNT number (N) at position L and the CNT number (n) with length L can be expressed as

$$N = N_0\alpha^{(L-1)} \quad (4)$$

$$n = N_0\alpha^{(L-1)}(1-\alpha) \quad (5)$$

The theoretical length distribution of ultralong CNTs is shown in Figure 2. A low α indicates the growth can be easily terminated, resulting in a low percentage of very long CNTs (Figure 2a). No matter for what α, the number density of ultralong CNTs decreases with their length increase (Figure 2b). The higher the α is, the slower the number density decreasing rate is. It should be noted that the length distribution of vertically aligned CNT arrays cannot be interpreted by SF distribution (see Supporting Text S2).

Figure 3a is typical mosaic SEM images of ultralong CNTs. The CNT number decreases along their axial direction (Figure 3b). The statistical numbers of both the total CNTs and the CNTs with a certain length fit well with the theoretical values. For the sample shown in Figure 2a, N_0 = 126, which means that there are 126 CNTs at L of 1 mm. On the basis of the unit length of 1 mm, we obtain α = 0.921. α can also be calculated according to eq 3. It should be noted that this analysis is based on statistics; consequently, a large CNT sampling number is highly required to demonstrate such distribution. Figure 3 panels c and d show four different number density and relative percentage distributions of ultralong CNTs (for similar distributions also see Supporting Information, Figure S1). All the experimental results are in good accordance with the theoretical values.

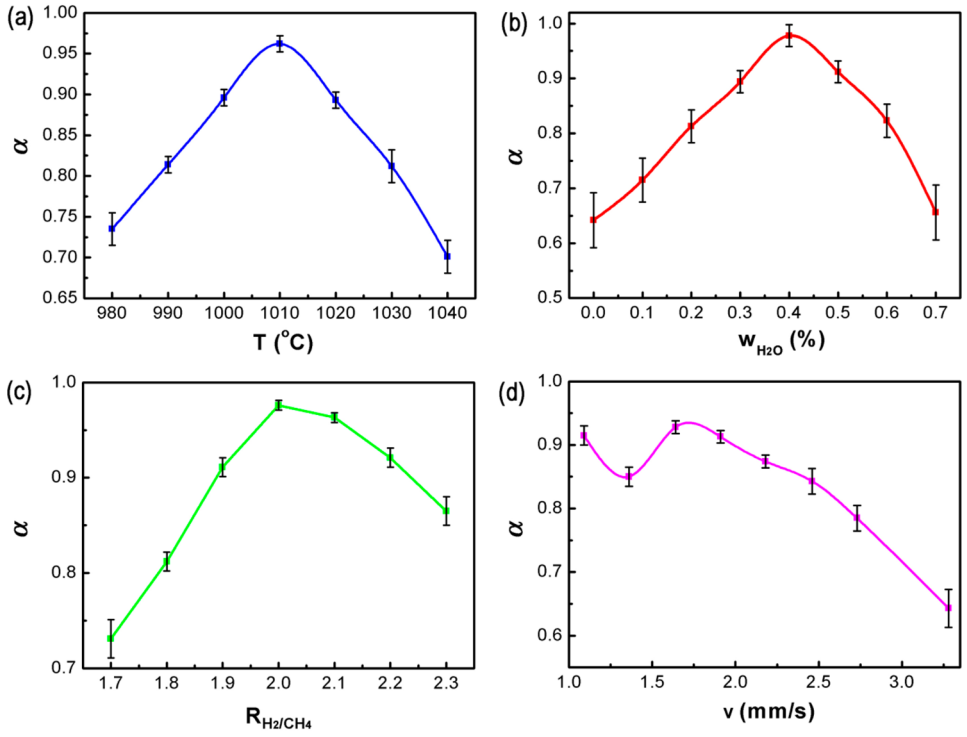

Figure 4. Relationship between catalyst activity probability (α) and different process parameters. (a) Relationship between α and growth temperature. (b) Relationship between α and water content. (c) Relationship between α and H_2/CH_4 ratio. (d) Relationship between α and gas velocity.

The catalyst activity is influenced by many factors, such as catalyst composition, sizes, growth temperature, carbon feedstock, substrates, flow field, space velocity, *etc*. The effect of operation parameter on catalyst activity were also explored. The growth temperature has a direct influence on catalyst activity (Figure 4a). At low temperature, catalysts have a weak activity, making the growth of ultralong CNT easily terminated. With increasing temperature, the catalyst activity improves accordingly. However, when the temperature is too high, the thermal cracking decomposition of carbon sources becomes rapid, and thus plenty of amorphous carbon forms on the catalyst surface, leading to decreased catalyst activity. The feedstock also plays an important role in catalyst activity. Ethanol and methane are the most widely employed carbon sources for synthesizing ultralong CNTs. The purity of feedstock should also be taken into consideration. Besides, it has been proven that adding a trace amount of water can significantly improve the growth of ultralong CNTs because water can effectively remove the deposited amorphous carbon on catalysts.[17] Water concentration has a direct impact on catalyst activity (Figure 4b). Low water concentration cannot effectively remove all the amorphous carbon deposited on the catalysts, while too much water removes not only the amorphous carbon but also other kinds of carbon thus decreasing the carbon supply. In addition, the ratio of H_2 to CH_4 also influences catalyst activity (Figure 4c). The ratio of H_2 to CH_4 mainly affects chemical equilibrium during CNT growth, which then affects the catalyst activity. In addition, gas velocity has a direct relationship with the Renault number and Richardson number of gas flow,[14] which influence the floating of growing CNTs. With the synergistic effects of Renault number and Richardson number, gas velocity has a complicated influence on α (Figure 4d). Besides, the gas velocity also affects the carbon feedings, especially when the gas velocity is very low. As for the substrates, they mainly affect the growth mode and the interaction between substrates and catalysts. It has been proven that silicon substrates are effective for the tip-growth mode of ultralong CNTs,[13,15,16,21] while quartz or sapphire substrates usually lead to the base-growth mode of CNTs.[30,32] Ultralong CNTs with different length distribution were obtained by varying these growth conditions (Supporting Information, Figure S4). Besides, a furnace with a long enough constant temperature zone must be used to enable the continuous growth of long CNTs. We proposed a "furnace-moving" method to obtain an ultralong heating zone (Supporting Information, Figure S5).

For synthesizing ultralong CNTs with high number density and length, the key is to improve the α value to be as high as possible. Figure 2a shows that even when α = 0.9/mm, the percentage of CNTs with length over 50 mm is only 0.001. Thus, to synthesis ultralong CNTs with length over 100 mm, α should be improved as high as possible. With the optimized growing windows and the furnace-moving method,

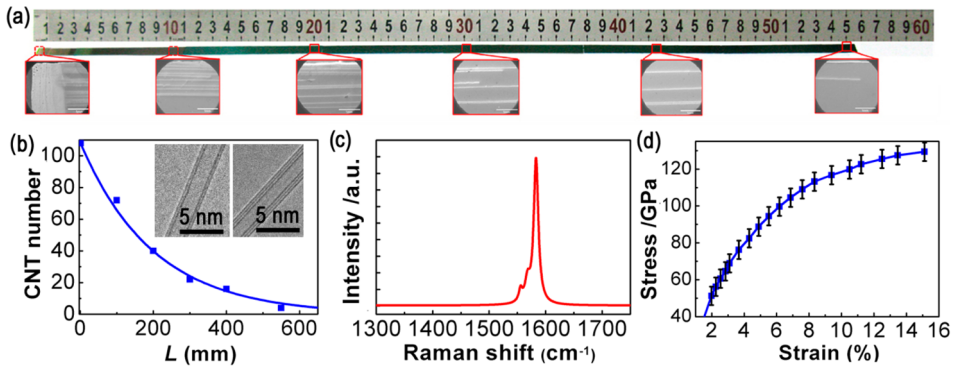

Figure 5. Synthesis and properties of 550-mm-long CNTs. (a) SEM image of 550 mm long CNTs. (b) Number of CNTs at different length on the substrate. Inset: TEM images of as-grown CNTs. (c) Raman spectrum of as-grown CNTs. (d) Mechanical properties of as-grown CNTs.

CNTs with length up to 550-mm were synthesized (Figure 5a). In this process, α was up to 0.995 (Figure 5b). For a single-walled CNT with diameter of 1 nm, α_{mm} = 0.995 means the catalyst deactivation probability for adding one carbon dimer is only 8.35×10^{-11} (see Supporting Text S3). This implies the feedstock has a very high purity. The ultralow catalyst deactivation also renders the as-grown ultralong CNTs as having perfect structures (inset in Figure 5b). There is no visible D-band (~1350 cm^{-1}) in the Raman spectrum of as-grown CNTs (Figure 5c), clearly showing their perfect structures. In addition, we also measured their mechanical properties using a "gas-flow" method reported before.[8] As shown in Figure 5d, the tensile stress of a CNT was up to 120 GPa and the breaking strain was up to 15%; both of the values reached theoretical values.

CONCLUSIONS

We report that SF distribution could well interpret the length distribution of ultralong CNTs. SF distribution implies that shorter CNTs are favored over longer ones. All the factors affecting the growth of ultralong CNTs could be integrated into catalyst activity probability. High catalyst activity probability will lead to long CNTs with high number density. By optimizing the growing parameters and applying a "furnace-moving" method, 550 mm-long CNTs with perfect structures were synthesized. This study shed new light on the understanding and rational design of growth process of ultralong CNTs.

MATERIALS AND METHODS

Synthesis of Ultralong CNTs with Different Conditions. The substrates were silicon slices (5−10 cm long, 0.5−1 cm wide, and 0.5 mm thick) with a 500 nm thick SiO_2 layer. The growth of CNTs was conducted in a quartz tube (inner diamter: 31 mm). $FeCl_3$ ethanol solution (0.001−0.1 mol·L^{-1}) was used as catalyst precursor and deposited onto substrates by a microprinting method. After reduction in H_2 and Ar (V_{H_2}:V_{Ar} = 2:1; F_{total} = 150 sccm) at 910 °C for 15 min, the temperature was increased from 910 °C to 970−1050 °C in three minutes. Then CH_4 and H_2 (V_{CH4}:V_{H2} =1:1.5−1:2.5; F_{total} = 50−200 sccm, with 0−0.7% H_2O) were inleted into the reactor for the growth of CNTs. The growth time was in the range of 10−120 min.

Measurement of CNT Growth Speed. The CNTs were synthesized with different growth time, for example, 5 min, 10 min, 15 min, 20 min, *etc.*. For CNTs with different length on substrates, only the longest 10 CNTs were taken into consideration for calculating growth speed. The average length of the 10 CNTs were taken as the CNT length at a given growth time.

Synthesis of 550 mm Long CNTs. The synthesis of 550 mm long CNTs was conducted in a furnace with a heating zone of 35 cm. The procedures were similar to the above: T = 1010 °C, v = 1.58 mm s^{-1}, c_{cat} = 0.5 mol L^{-1}, w_{H_2O} = 0.4%, and R_{H_2/CH_4} = 2. The furnace was fixed with four wheels on two parallel tracks. A motor was fixed to make the furnace move at a given speed. The growth speed of ultralong CNTs was about 5 mm/s, so the moving speed of the furnace was also set to 5 mm s^{-1}. After the introduction of CH_4 and H_2 into the quartz tube at 1010 °C, the motor was turned on and the furnace started to move. The growth duration was 2 h.

Conflict of Interest: The authors declare no competing financial interest.

Supporting Information Available: Supporting figures and supporting texts as described in the text. This material is available free of charge *via* the Internet at http://pubs.acs.org.

Acknowledgment. The work is supported by the Foundation for the National Basic Research Program of China (2011CB932602, 2013CB934200) and the National Science Foundation of China (21203107).

REFERENCES AND NOTES

1. Flory, P. J. Molecular Size Distribution in Linear Condensation Polymers. *J. Am. Chem. Soc.* **1936**, *58*, 1877–1885.
2. Flory, P. J. *Principles of Polymer Chemistry*; Cornell University Press: Ithica, NY, 1953; Vol. 1.
3. Bianchini, C.; Giambastiani, G.; Guerrero, I. R.; Meli, A.; Passaglia, E.; Gragnoli, T. Simultaneous Polymerization and Schulz−Flory Oligomerization of Ethylene Made Possible by Activation with MAO of a C1-Symmetric [2, 6-Bis (arylimino) pyridyl] Iron Dichloride Precursor. *Organometallics* **2004**, *23*, 6087–6089.
4. McGuinness, D. S.; Wasserscheid, P.; Morgan, D. H.; Dixon, J. T. Ethylene Trimerization with Mixed-Donor Ligand (N, P, S) Chromium Complexes: Effect of Ligand Structure on Activity and Selectivity. *Organometallics* **2005**, *24*, 552–556.

5. Zhang, X.; Wang, J. An Alternative Deductive Method for Molecular Weight Distribution Function of Linear Polymers. *Acta Polym. Sin.* **2005**, *5*, 725–730.
6. Aravind, R.; Kunzru, D.; Gupta, S. K. Vapor Grown Carbon Fibers: Modeling of Filament Length Distributions. *J. Anal. Appl. Pyrol.* **1994**, *28*, 255–270.
7. Gupta, S. K.; Gupta, N.; Kunzru, D. Vapor Grown Carbon Fibers From Pyrolysis of Hydrocarbons: Modeling of Filament Growth and Poisoning. *J. Anal. Appl. Pyrol.* **1993**, *26*, 131–144.
8. Zhang, R.; Wen, Q.; Qian, W.; Su, D. S.; Zhang, Q.; Wei, F. Superstrong Ultralong Carbon Nanotubes for Mechanical Energy Storage. *Adv. Mater.* **2011**, *23*, 3387–3391.
9. Yu, M. F.; Lourie, O.; Dyer, M. J.; Moloni, K.; Kelly, T. F.; Ruoff, R. S. Strength and Breaking Mechanism of Multiwalled Carbon Nanotubes under Tensile Load. *Science* **2000**, *287*, 637–640.
10. Peng, B.; Locascio, M.; Zapol, P.; Li, S.; Mielke, S.; Schatz, G.; Espinosa, H. Measurements of Near-Ultimate Strength for Multiwalled Carbon Nanotubes and Irradiation-Induced Crosslinking Improvements. *Nat. Nanotechnol.* **2008**, *3*, 626–631.
11. Edwards, B. C. Design and Deployment of a Space Elevator. *Acta Astron.* **2000**, *47*, 735–744.
12. Wen, Q.; Qian, W.; Nie, J.; Cao, A.; Ning, G.; Wang, Y.; Hu, L.; Zhang, Q.; Huang, J.; Wei, F. 100 mm Long, Semiconducting Triple-Walled Carbon Nanotubes. *Adv. Mater.* **2010**, *22*, 1867–1871.
13. Wang, X. S.; Li, Q. Q.; Xie, J.; Jin, Z.; Wang, J. Y.; Li, Y.; Jiang, K. L.; Fan, S. S. Fabrication of Ultralong and Electrically Uniform Single-Walled Carbon Nanotubes on Clean Substrates. *Nano Lett.* **2009**, *9*, 3137–3141.
14. Peng, B. H.; Yao, Y. G.; Zhang, J. Effect of The Reynolds and Richardson Numbers on The Growth of Well-Aligned Ultra Long Single-Walled Carbon Nanotubes. *J. Phys. Chem. C* **2010**, *114*, 12960–12965.
15. Liu, Y.; Hong, J. X.; Zhang, Y.; Cui, R. L.; Wang, J. Y.; Tan, W. C.; Li, Y. Flexible Orientation Control of Ultralong Single-Walled Carbon Nanotubes by Gas Flow. *Nanotechnology* **2009**, 20.
16. Jin, Z.; Chu, H. B.; Wang, J. Y.; Hong, J. X.; Tan, W. C.; Li, Y. Ultralow Feeding Gas Flow Guiding Growth of Large-Scale Horizontally Aligned Single-Walled Carbon Nanotube Arrays. *Nano Lett.* **2007**, *7*, 2073–2079.
17. Wen, Q.; Zhang, R. F.; Qian, W. Z.; Wang, Y. R.; Tan, P. H.; Nie, J. Q.; Wei, F. Growing 20 cm Long DWNTs/TWNTs at a Rapid Growth Rate of 80−90 μm/s. *Chem. Mater.* **2010**, *22*, 1294–1296.
18. Yao, Y.; Li, Q.; Zhang, J.; Liu, R.; Jiao, L.; Zhu, Y.; Liu, Z. Temperature-Mediated Growth of Single-Walled Carbon-Nanotube Intramolecular Junctions. *Nat. Mater.* **2007**, *6*, 283–286.
19. Zheng, L.; O'connell, M.; Doorn, S.; Liao, X.; Zhao, Y.; Akhadov, E.; Hoffbauer, M.; Roop, B.; Jia, Q.; Dye, R. Ultralong Single-Wall Carbon Nanotubes. *Nat. Mater.* **2004**, *3*, 673–676.
20. Hong, B. H.; Lee, J. Y.; Beetz, T.; Zhu, Y. M.; Kim, P.; Kim, K. S. Quasi-Continuous Growth of Ultralong Carbon Nanotube Arrays. *J. Am. Chem. Soc.* **2005**, *127*, 15336–15337.
21. Reina, A.; Hofmann, M.; Zhu, D.; Kong, J. Growth Mechanism of Long and Horizontally Aligned Carbon Nanotubes by Chemical Vapor Deposition. *J. Phys. Chem. C* **2007**, *111*, 7292–7297.
22. Zheng, L. X.; Satishkumar, B. C.; Gao, P. Q.; Zhang, Q. Kinetics Studies of Ultralong Single-Walled Carbon Nanotubes. *J. Phys. Chem. C* **2009**, *113*, 10896–10900.
23. Liu, H. P.; Takagi, D.; Chiashi, S.; Homma, Y. The Controlled Growth of Horizontally Aligned Single-Walled Carbon Nanotube Arrays by a Gas Flow Process. *Nanotechnology* **2009**, *20*, 345604.
24. Huang, S. M.; Woodson, M.; Smalley, R.; Liu, J. Growth Mechanism of Oriented Long Single Walled Carbon Nanotubes Using "Fast-Heating" Chemical Vapor Deposition Process. *Nano Lett.* **2004**, *4*, 1025–1028.
25. Yakobson, B. I.; Harutyunyan, A. R.; Feng, D. Dislocation Theory of Chirality-Controlled Nanotube Growth. *Proc. Natl. Acad. Sci. U.S.A.* **2009**, *106*, 2506–2509.
26. Marchand, M.; Journet, C.; Guillot, D.; Benoit, J. M.; Yakobson, B. I.; Purcell, S. T. Growing a Carbon Nanotube Atom by Atom: "And Yet It Does Turn". *Nano Lett.* **2009**, *9*, 2961–2966.
27. Wijeratne, S. S.; Harris, N. C.; Kiang, C. H. Helicity Distributions of Single-Walled Carbon Nanotubes and Its Implication on the Growth Mechanism. *Materials* **2010**, *3*, 2725–2734.
28. Morin, S. A.; Bierman, M. J.; Tong, J.; Jin, S. Mechanism and Kinetics of Spontaneous Nanotube Growth Driven by Screw Dislocations. *Science* **2010**, *328*, 476–480.
29. Li, Y.; Cui, R. L.; Ding, L.; Liu, Y.; Zhou, W. W.; Zhang, Y.; Jin, Z.; Peng, F.; Liu, J. How Catalysts Affect the Growth of Single-Walled Carbon Nanotubes on Substrates. *Adv. Mater.* **2010**, *22*, 1508–1515.
30. Su, M.; Li, Y.; Maynor, B.; Buldum, A.; Lu, J. P.; Liu, J. Lattice-Oriented Growth of Single-Walled Carbon Nanotubes. *J. Phys. Chem. B* **2000**, *104*, 6505–6508.
31. Ding, L.; Tselev, A.; Wang, J. Y.; Yuan, D. N.; Chu, H. B.; McNicholas, T. P.; Li, Y.; Liu, J. Selective Growth of Well-Aligned Semiconducting Single-Walled Carbon Nanotubes. *Nano Lett.* **2009**, *9*, 800–805.
32. Ismach, A.; Segev, L.; Wachtel, E.; Joselevich, E. Atomic-Step-Templated Formation of Single Wall Carbon Nanotube Patterns. *Angew. Chem., Int. Ed.* **2004**, *116*, 6266–6269.